An AVO Primer

By
Brian Russell[1]

Search and Discovery Article #40051 (2002)

*Adapted for online presentation from an article by the same author in *AAPG Explorer* (June, 1999), entitled "AVO Adds Flavor to Seismic Soup." Appreciation is expressed to the author and to M. Ray Thomasson, former Chairman of the AAPG Geophysical Integration Committee, and Larry Nation, AAPG Communications Director, for their support of this online version.

[1]Hampson-Russell Software Services Ltd., Calgary, Canada (www.hampson-russell.com; brian@hampson-russell.com); past president of the Society of Exploration Geophysicists.

General Statement

AVO, which stands for Amplitude Variations with Offset--or, more simply, Amplitude Versus Offset--is a seismic technique that looks for direct hydrocarbon indicators using the amplitudes of prestack seismic data. The basics of the AVO method will be explained here using the two geological models shown in Figure 1:

- Figure 1a shows a brine-filled sand pinchout encased in shale.
- Figure 1 b displays the same sand saturated with gas.

Wells have been drilled into each sand.

P- and S Waves

To understand the AVO effects of these two models, we must first discuss seismic waves and the recording of seismic data. Traditional seismic data are recorded using compressional waves, or P-waves, which move through the earth by alternately, compressing and expanding the rocks in their direction of propagation. However, there is a second type of wave called a shear wave, or S-wave, which travels by shearing the rocks at right angles to its direction of propagation. This is illustrated in Figure 2.

There are several important differences between P- and S-waves:

- First, the velocity of the S-wave is slower than the velocity of the P-wave for a given geological formation.
- Second, S-waves are less sensitive to the presence of gas in a reservoir than P-waves. since the high compressibility of gas has more of an effect on the Pwave velocity.
- A third important physical parameter is the density that is strongly affected by the presence of gas.

Figures 3 and 4 show the P-wave velocity, S-wave velocity and density logs for the two models of Figure 1. Notice that both the P-wave velocity and the density are lower in the gas sand than in the wet sand, but the S-wave velocity is the same in both cases. To understand how this is related to the recorded seismic trace, note that the seismic recording measures two things: the time that it takes to travel down to a particular geological interface, and the reflection amplitude.

Figures 3 and 4 also show how the amplitudes are created. First, we multiply the velocity times the density to get the P or S impedance. Then, we calculate the difference between the impedances divided by their sum, which gives us a reflection coefficient (reflectivity) at each interface. Finally, we superimpose the seismic response, or wavelet, on the reflection

coefficients to get the synthetic seismic traces shown at the far right of both figures.

The P and S synthetics for the wet model are almost identical, but for the gas model the S-wave synthetic is the reverse of the P-wave synthetic and has lower amplitudes. The high amplitude reflections seen on the P-wave response of the gas model are called "bright-spots," and can be effective in the Gulf Coast and other areas in the search for gas sands. Figure 5 shows such a bright-spot reflection from a shallow Cretaceous play in Alberta at 640 msec.

However, there are other geological situations that create 'bright-spots," such as coal seams or hard streaks. From this discussion, it is obvious that the P-wave response does not reveal the presence of gas unambiguously, and it needs to be supplemented with an S-wave recording. Unfortunately, S-wave recording is not that common. This leads us to the AVO method, which allows us to derive a similar result without actually recording an S-wave section.

The AVO Method

Figure 6, which shows a typical prestack seismic raypath, records that the incident wave displays both compressional and shear effects, since it strikes the interface at an angle a. The reflected wave thus contains the effects of both P- and S-waves. Although the mathematics of this process has been known since the nineteenth century, it was only very recently that we have recognized it on our seismic data. Ostrander (1984) showed that, for the simple model of Figure 1b, the amplitudes on a prestack gather would increase with offset. This is shown in Figure 7, in which the reflections from the gathers (seismic traces from one point displayed side by side) over the shallow gas sand of Figure 6 are seen quite clearly to increase.

Not all gas sands show increasing AVO effects, since the result is dependent on the nature of the acoustic impedance change. The different types of AVO anomalies have been classified as classes 1, 2 and 3 by Rutherford and Williams (1989} In the present paper we are looking at a Class 3 example, in which the impedance of the sand is lower than the encasing shale.

If we measure the amplitude of each reflection amplitude as a function of offset, and plot them on a graph as a function of the sine of angle of incidence squared, we observe a straight line. For any line, the intercept and gradient can be measured. By linearizing the complicated mathematics behind the AVO technique, Richards and Frasier (1976) and Wiggins et al (1986) gave us the following physical interpretation of the intercept and gradient:

Intercept = the P-wave reflection amplitude.

Gradient = the P-wave reflection amplitude minus twice the S-wave reflection amplitude.

To illustrate this point, the amplitudes from a small portion of one of the gathers in Figure 7 are shown in Figure 8, with a straight line fit superimposed. Notice that the top of the sand has a negative intercept (a trough) and a negative gradient, and the base of the sand has a positive intercept (peak) and a positive gradient. When we perform this analysis at every sample, on every gather, we create two sections, or volumes. The intercept section is similar to the conventional stack--except that it represents a better estimate of the vertical P-wave reflections. The gradient contains

information about both the P and S-wave reflections.

There are many ways of displaying this information. As well as displaying the intercept and gradient on their own, it is common to display the difference and sum of the intercept and gradient. From the above explanation it is obvious that the difference, after scaling, is the approximate S-wave reflectivity. The sum of the intercept and the gradient can be shown to represent the approximate Poisson's ratio change, where Poisson's ratio is related to the square of the P-wave to S-wave velocity ratio. A negative Poisson's ratio change is associated with the top of a gas zone, whereas a positive change is associated with the base.

These displays are shown in Figures 9 and 10 for our real example. Notice that the intercept (P-wave) shows a strong "bright-spot," whereas the pseudo-S-wave (intercept minus gradient) does not show a "bright-spot," indicating the presence of a gas sand.

As one final example, let us consider an example of the AVO technique applied to 3-D data. Figure 11 shows the sum of intercept and gradient, or pseudo-Poisson's ratio computed over the top of a channel sand in Alberta. The negative values on this plot indicate the possible presence of gas in the channel sand.

Conclusion

This tutorial has reviewed the basic principles behind the AVO technique. We have concentrated on a single type of anomaly, the Class 3, in which the acoustic impedance of the gas sand drops with respect to the encasing shales. For a discussion of other types of anomalies refer to the papers by Rutherford and Williams (1989), Ross and Kinman (1995). and Verm and Hilterman (1995).

The key thing to remember about the AVO method is that the AVO gradient responds to both P- and S-wave reflections from an interface, and this behavior can be used to locate gas charged reservoirs. Applied to 3-D seismic data, the AVO technique gives us a robust and inexpensive method for identifying potential reservoirs and is a technique that adds an extra dimension to studies done only with stacked seismic data

References

Ostrander, W.J., 1984, Plane-wave reflection coefficients for gas sands at nonnormal angles of incidence: Geophysics, v. 49, p. 1637-1648.

Richards, P.G., and Frasier, C.W., 1976, Scattering of eleastic waves from depth-dependent inhomogeneities: Geophysics, v. 41, p. 441-458.

Ross, C.P., and Kinman, D.L., 1995, Nonbright-spot AVO; two examples: Geophysics, v. 60, p. 1398-1408.

Rutherford, S.R., and Williams, R.H., 1989, Amplitude-versus-offset variations in gas sands: Geophysics, v. 54, p. 680-688.

Verm, R., and Hilterman, F., 1995, Lithology, color-coded siesmic sections; the calibration of AVO crossplotting to rock properties: Leading Edge, v. 14, p. 847-853.

Wiggins, W., Ng, P., and Manzur, A., 1986, The relation between the VSP-CDP transformation and VSP migration (abstract): SEG Abstracts, v. 1, p. 565-568.

Figures

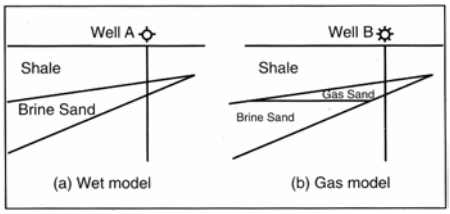

Figure 1. Two geological models that will illustrate the basics of the AVO method.

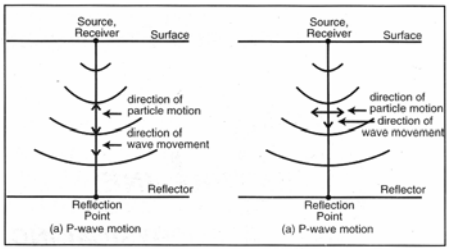

Figure 2. A simple drawing of P- and S-wave motion.

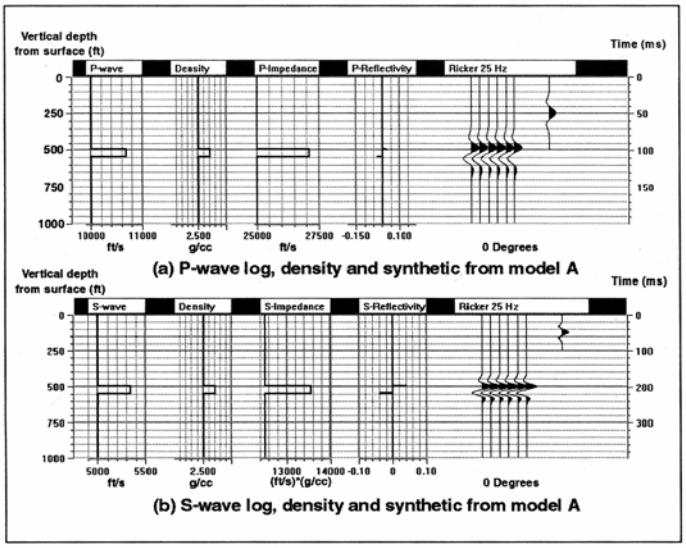

Figure 3. The velocities, densities and synthetic seismograms for model A.

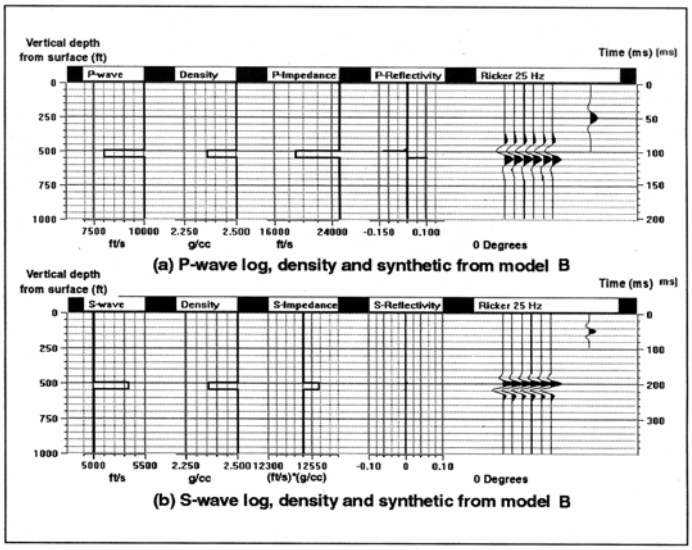

Figure 4. The velocities, densities and synthetic seismograms for model B.

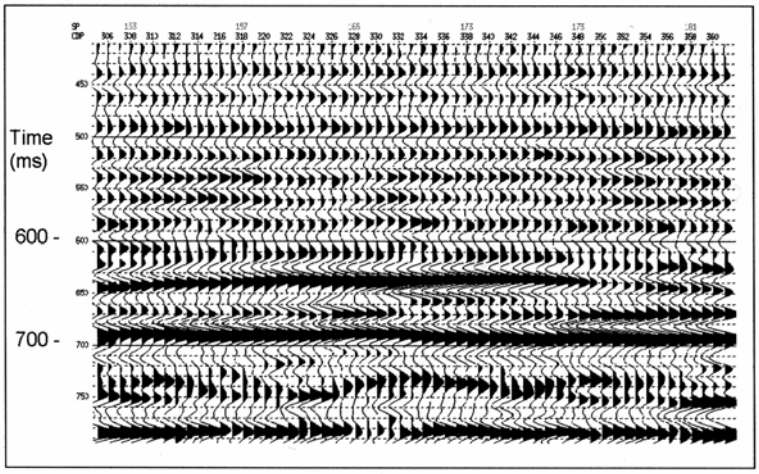

Figure 5. A stacked section from Alberta showing a "bright-spot" at 640 msec caused by a Cretaceous gas sand.

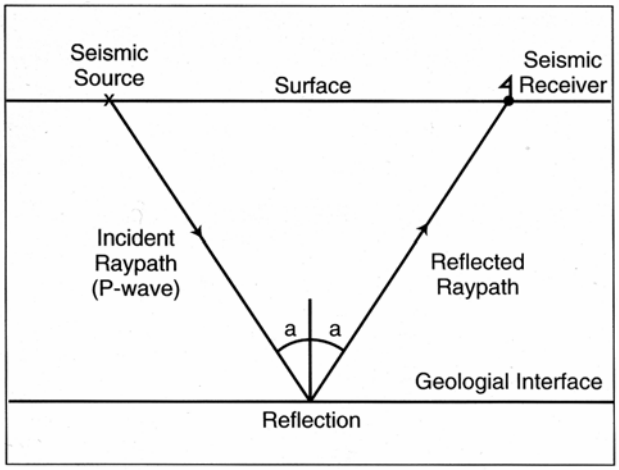

Figure 6. The geometry of a reflected P-wave at a given angle a. The offset is the distance from the source to the receiver.

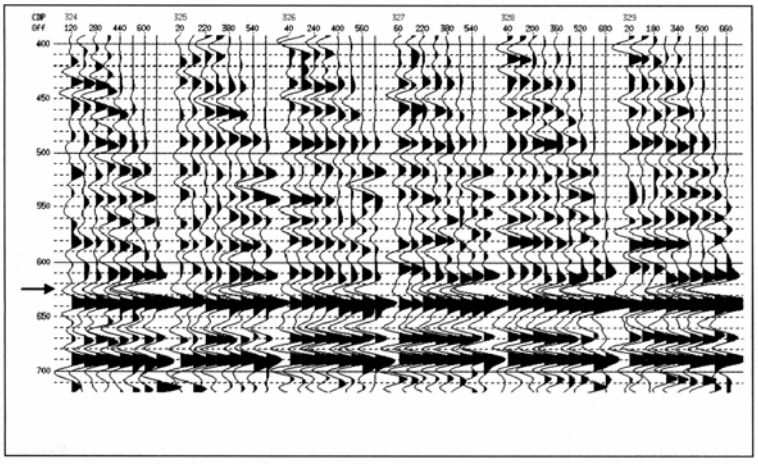

Figure 7. The CDP gathers from a portion of the stacked section in Figure 6, over the "bright-spot". Notice the amplitude increase indicated at the zone shown by an arrow.

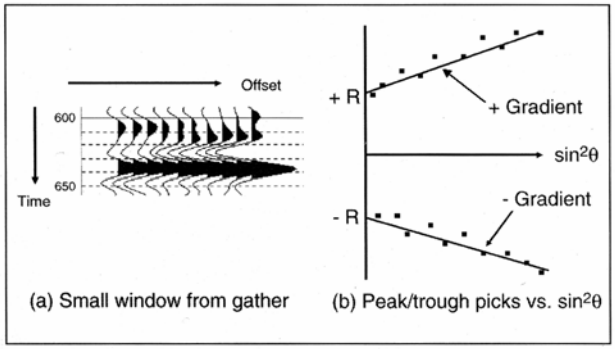

Figure 8. The intercept and gradient fit to the top and base reflections from a gas sand.

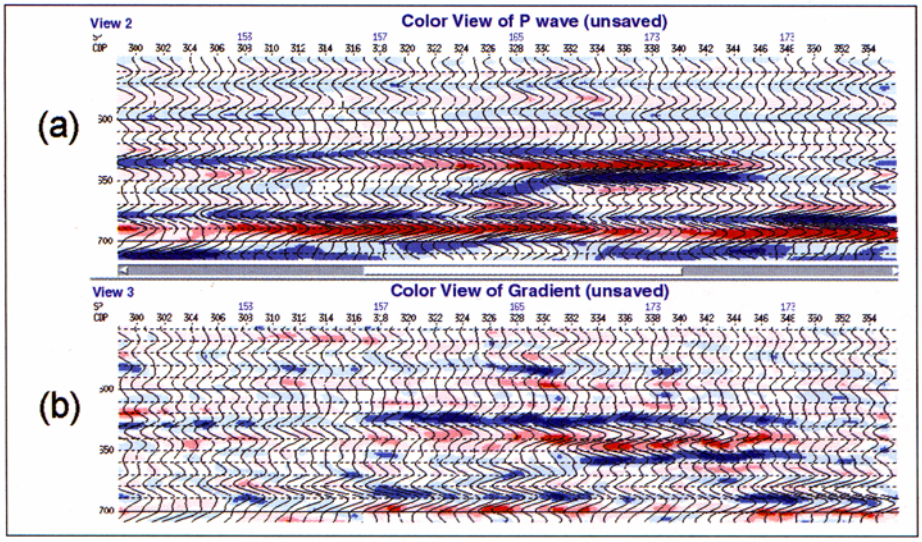

Figure 9. The intercept (a) and gradient (b) for the example shown in Figures 6 and 7.

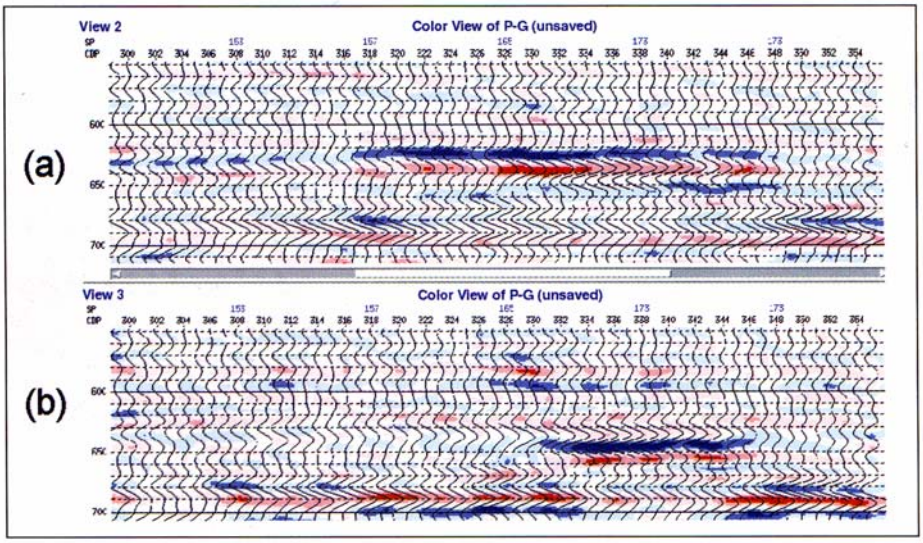

Figure 10. The sum (a) and difference (b) of the intercept and gradient shown in Figure 9.

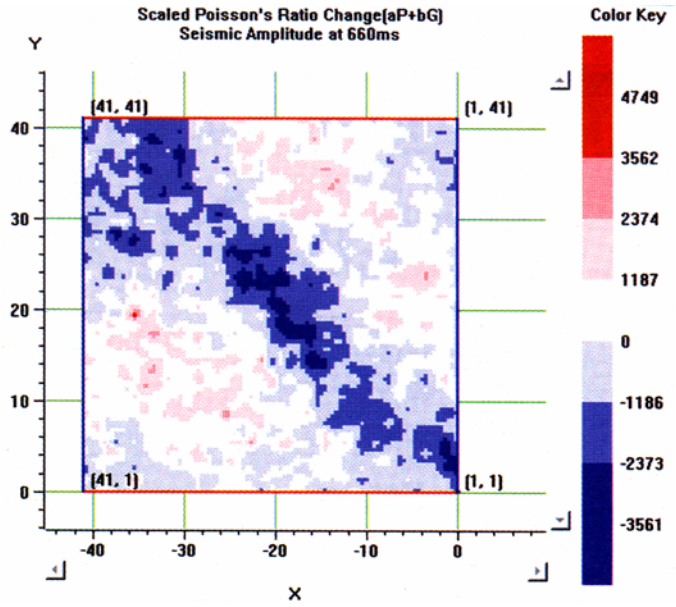

Figure 11. A 3D AVO example from a Cretaceous channel sand in Alberta. The plot shows the sum of intercept and gradient, or pseudo-Poisson's ratio.